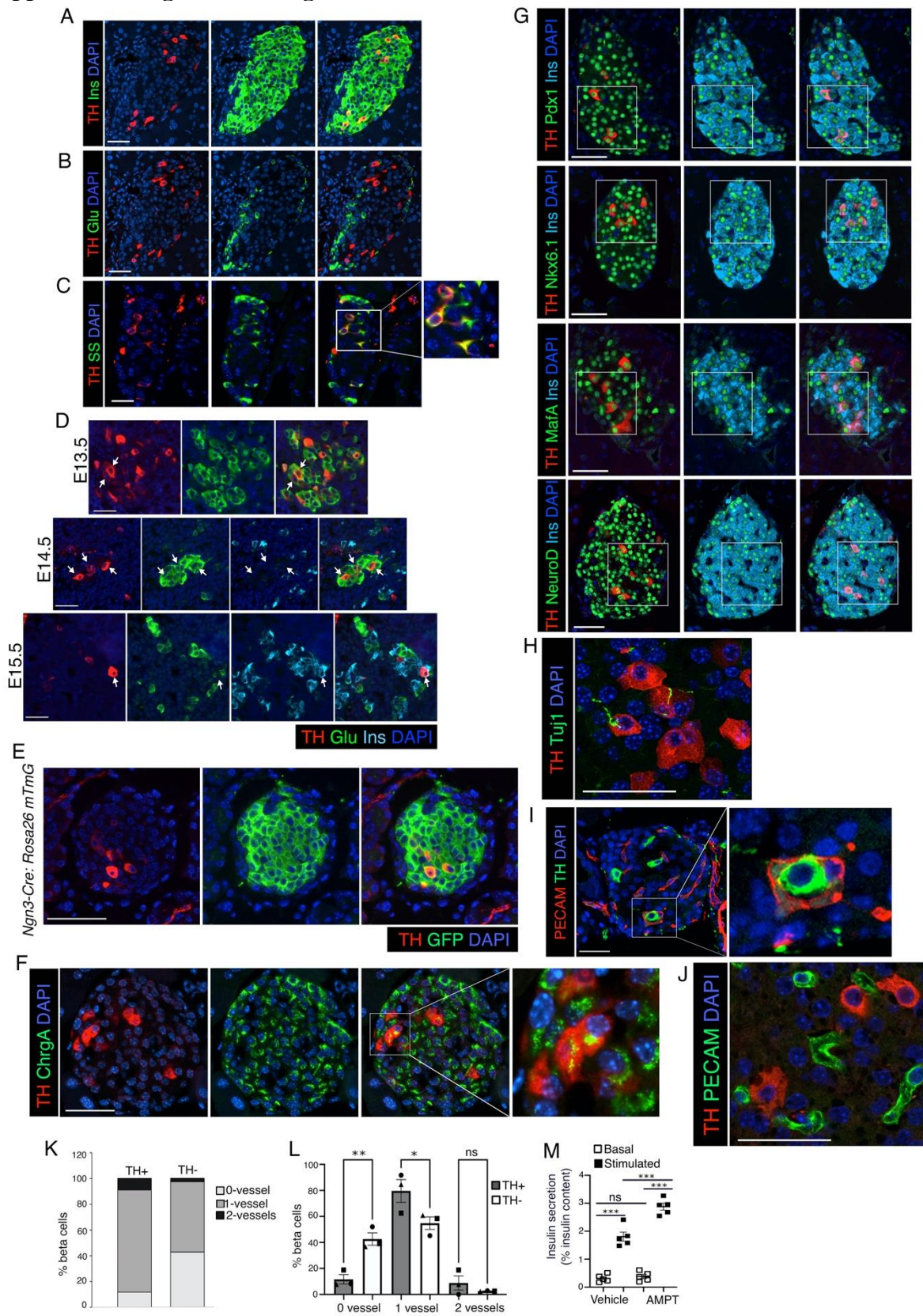
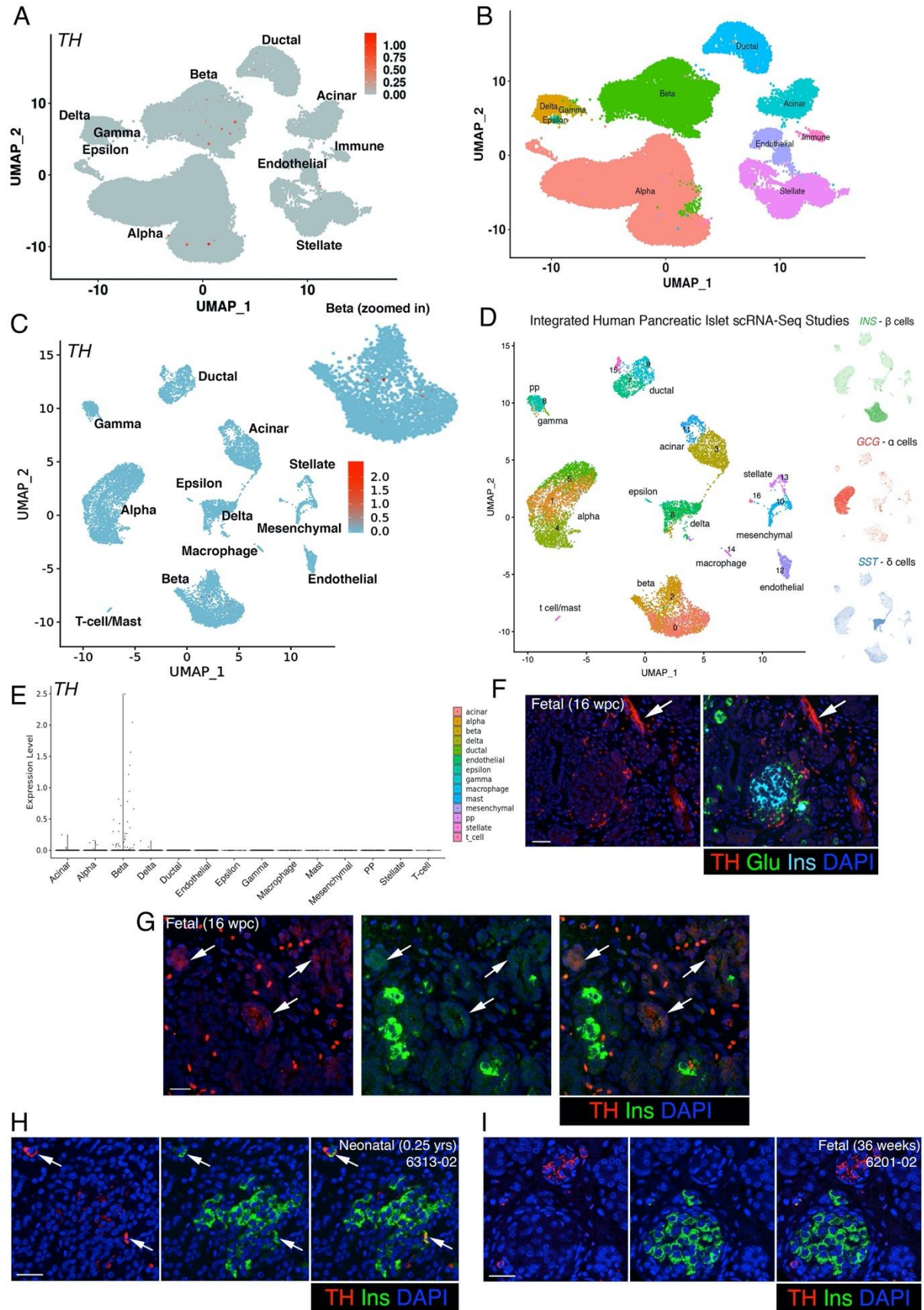


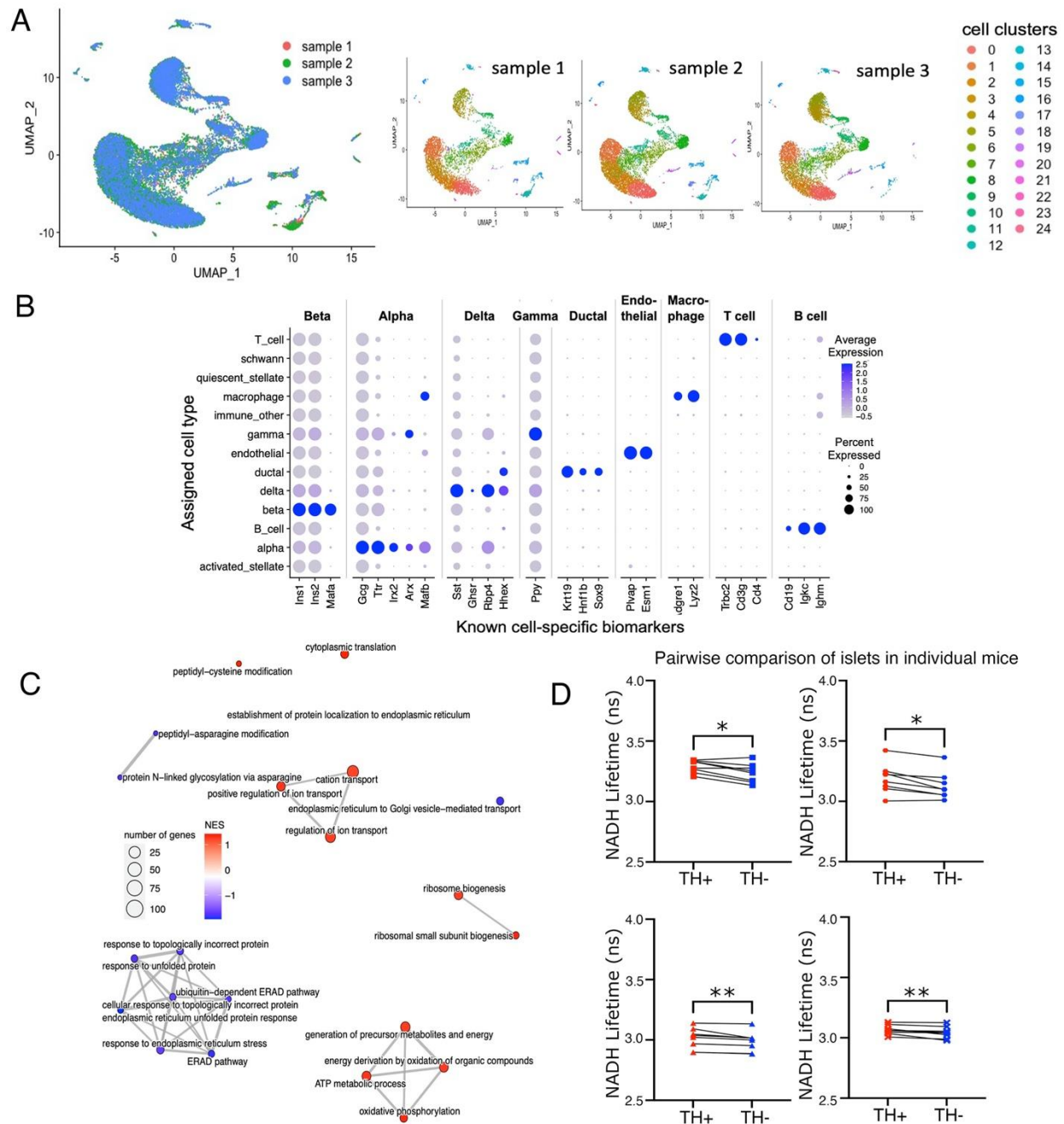
Supplemental Figures and Legends



Supplementary Figure 1 (Related to Figure 1). (A, B) Immunofluorescence analysis of adjacent pancreatic sections from adult wildtype mice (2 months old) for TH (red) and insulin (Ins: green) in (A), and TH (red) and glucagon (Glu: green) in (B), showing that TH overlaps with insulin but not glucagon in the adult islets. DAPI counter-stains the nuclei (blue). (C) Immunostaining for TH (red) and somatostatin (SS: green), with DAPI (blue), showing that TH also marks a fraction of adult delta cells. Right panel shows a 2X magnified view of the area marked by a white square. (D) Immunostaining for Tyrosine Hydroxylase (TH: red), glucagon (Glu: green), and Insulin (Ins: cyan), with DAPI in blue in embryonic pancreas at E13.5, E14.5, and E15.5. Arrows indicate cells co-expressing TH and Glu (top and middle panels; E13.5 and E14.5) or TH and Ins (bottom panel; E15.5). (E) Representative pancreatic sections from *Ngn3-Cre:Rosa26* mTmG lineage reporter mice at 2 months of age, stained for TH (red) and GFP (green) with DAPI in blue. (F) Immunostaining for TH (red) with chromogranin A (ChrgA : green), DAPI (blue). Panel on the far-right shows a 2.5X magnification of the area marked by white square. (G) Full, un-cropped images corresponding to Figure 1(G) for immunofluorescence analyses showing overlap of TH (red) with key transcription factor hallmarks of beta cell identity, namely, Pdx1 (top left), Nkx6.1 (top right), MafA (bottom left) and NeuroD1 (bottom right) shown in green. Nuclei are marked in blue with DAPI. The regions marked by white box are zoomed 2X and presented in Figure 1(G). (H) Immunostaining for TH (red) with sympathetic neuronal marker (shown in green) Tuj1 showing interaction of sympathetic afferents with TH-positive islet cells. (I) Immunostaining for TH (green) with PECAM1 (red). (J) Immunostaining for TH (red) with PECAM1 (green). Right panel shows a 2.5X magnification of the area in white box. (K, L) Quantification of PECAM1+ capillary contact with TH+ and TH- beta-cells (2000 beta-cells/slide, 2 slides spanning 100 μ m for each pancreas, n=4 pancreas), showing percentages of contact with 0, 1, or 2 capillaries (K), and comparison of each category between the TH+ and TH- beta-cells (L). (M) Static incubation GSIS in islets from 8 weeks old C57BL/6J mice, pretreated either with 10 μ M AMPT or vehicle (sterile 1X PBS) for 24 hours. For (A-C, F-J) representative pancreatic sections are shown from adult (2 months old), wildtype C57BL/6J mice, n=5 animals. Panel (C) shows representative images from n=5 wildtype C57BL/6J mouse embryos at indicated stages. Panels (E) shows representative data from (n=5) 2 months old *Ngn3-Cre:Rosa26* mTmG mice. (M) shows mean of islets from n=5 mice per group split into two pools for each treatment. The error bars represent standard error (SEM) of the mean. ns= not significant, * $P < 0.05$, ** $P < 0.01$, *** $P < 0.005$, determined by using a1-way ANOVA followed by a Fisher's LSD test for (L) and Šídák post-hoc test for (M). Scale bar: 50 μ m.

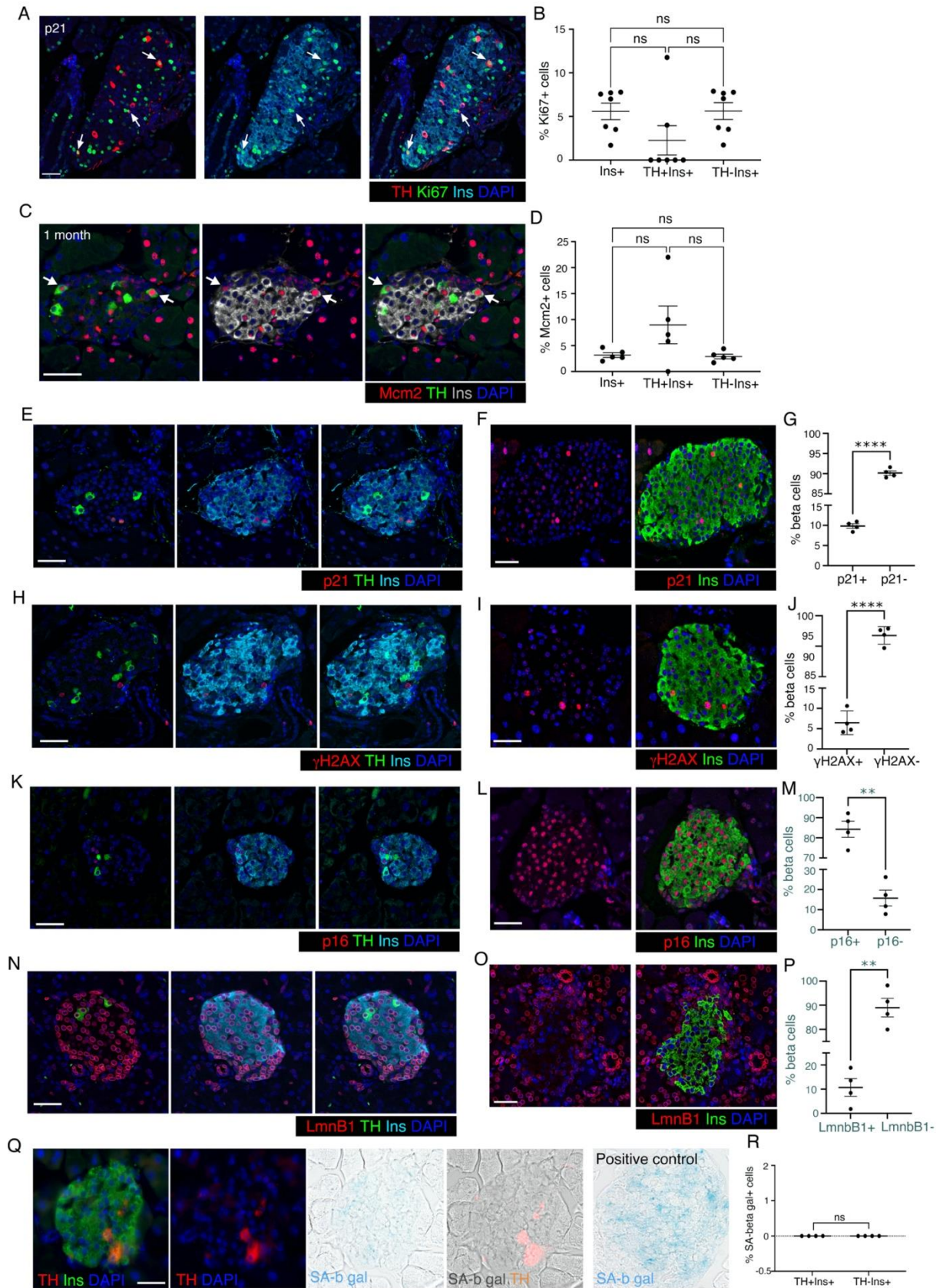


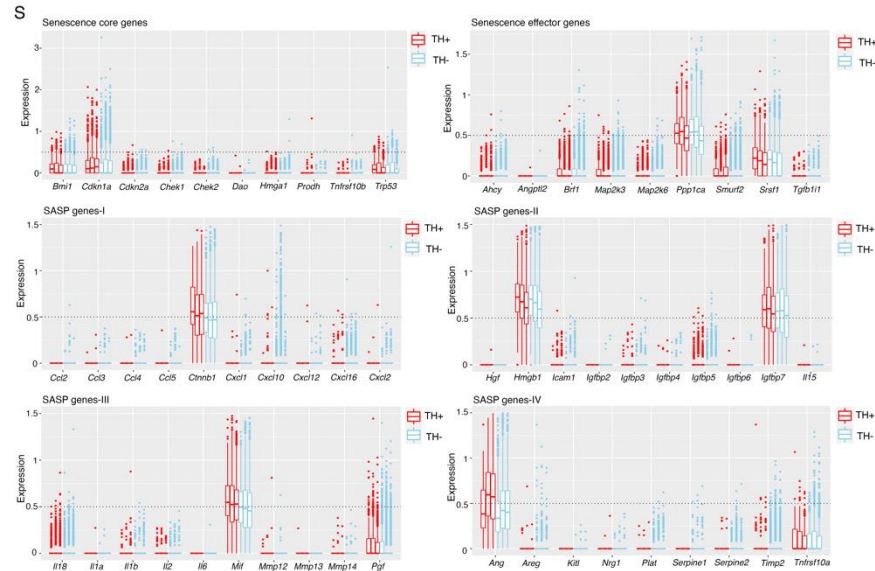
Supplementary Figure 2 (Related to Figure 2). (A, B) Data shows distribution of *TH* mRNA expression in different human islet cell populations in single-cell RNA sequencing (scRNA-seq) as a UMAP (Uniform Manifold Approximation and Projection) plot. This plot is derived from data resources made publicly accessible by (1) hosted at the authors' laboratory website (<https://powersbrissovalab.shinyapps.io/scRNAseq-Islets/#>). (C-E) Data shows distribution of *TH* mRNA expression in different human islet cell populations in single-cell RNA sequencing (scRNA-seq) data meta-analyzed and made publicly accessible by (2) https://www.huisinlab.com/diabetes_2019/index.html. The data shown is an integration of four human pancreatic islet datasets, as noted in the study. (C, D) show a UMAP (Uniform Manifold Approximation and Projection) plot, while (E) shows a violin plot. (F-I) Immunofluorescence images from fetal and neonatal human pancreas showing TH and Insulin (TH: red; Ins: green), DAPI (blue). (F, G) Representative images from n=1 early fetal human pancreas at 16 wpc, showing no TH+ beta-cells in endocrine cells within islets (F), while TH+ endocrine cells with faint insulin positivity can be easily observed in scattered clusters (G). (H, I) Representative examples from late fetal and neonatal human pancreas samples showing examples with (H), or without (I) TH+ beta-cells near islets. Arrows indicate TH+ beta-cells.



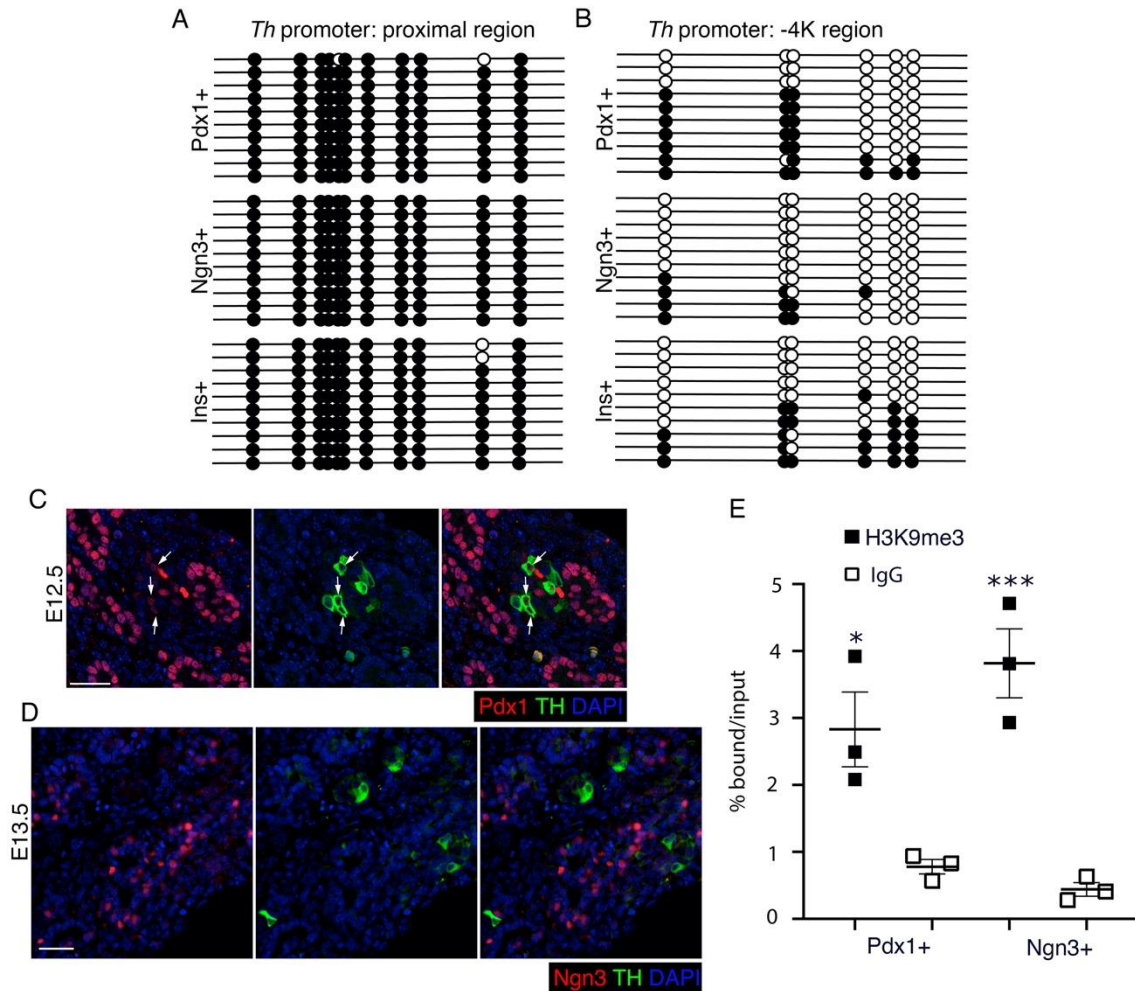
Supplementary Figure 3 (Related to Figure 3). (A) Overlay of the three replicate samples in the integrated dataset and depiction of the three samples individually in the UMAP space. The colors represent the cell clusters as identified by Seurat. (B) Validation of the assigned cellular types by SingleR. In this dotplot, the x axis represents the known biomarkers for each assigned cell type and the y axis represents the assigned cell types by SingleR. For each dot, the diameter is proportional to the percentage of cells expressing the specific gene, while the color intensity is proportional to the average expression in that cellular group. (C) Enriched pathways clustered into pathway modules based on their number of shared genes. Pathways that share many common genes are clustered together, where the edge thickness is proportional to the Jaccard similarity (fraction

of shared genes to the total number of genes in both pathways). Upregulated pathways (positive Normalized Enrichment Score - NES) are colored red, while downregulated pathways (NES , 0) are colored blue. comparison between *Th*⁺ and *Th*⁻ beta cells of the major beta cell clusters. The enrichment was calculated for Gene Ontology-Biological process (GO-BP) terms. (D) Pairwise comparison of NADH lifetime signatures for TH⁺ (red) vs TH⁻ (blue) beta-cells for individual islets in a single animal, shown for each of the four animals used. Error-bars show SEM. * $P < 0.05$, ** $P < 0.01$ using a paired *t*-test.

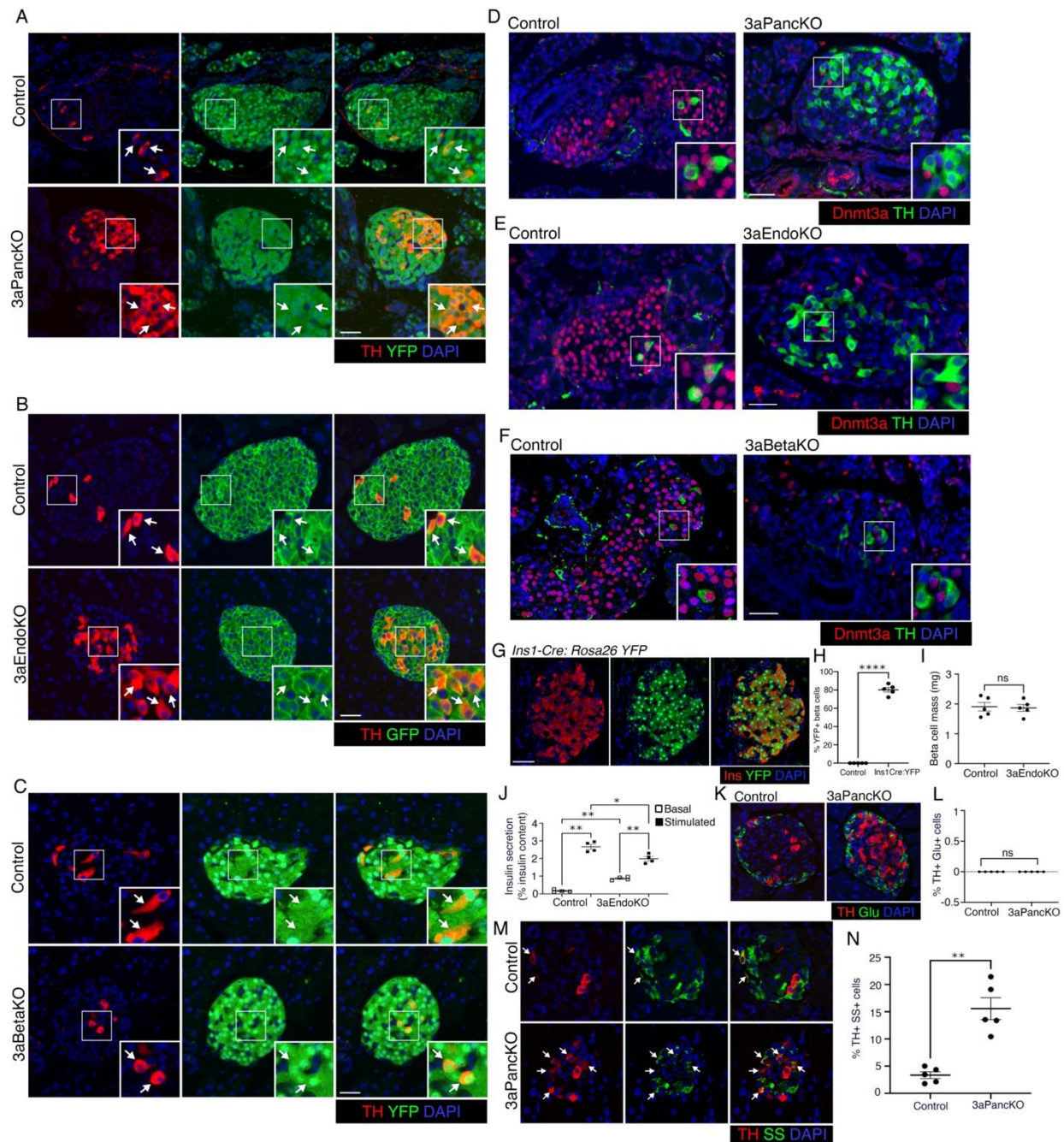




Supplementary Figure 4 (Related to Figure 4). (A, B) Immunostaining (A) and quantification (B) from $n=7$ pups at P21, for Ki67 (green), TH (red), insulin (cyan), with DAPI (blue) in total, TH+, and TH- beta-cells, expressed as a percentage of total cells in that population. (C, D) Immunostaining (C) and quantification (D) for replication licensing marker Mcm2 (red), along with TH (green) and insulin (Ins: grey) in 1 month old wildtype C57BL/6J mice ($n=5$). DAPI labels the nuclei in blue. (E-P) Representative immunofluorescence images showing uncropped single channel and merged views for various senescence markers in red (p21 in E, γ -H2AX in F, p16 in G, and LaminB1/LmnB1 in H), along with TH (green) and DAPI (blue), corresponding to Figure 4 F, H, J, and L, respectively. Panel F, G, I, J, L, M, O, P show representative images and the corresponding quantification for appropriate positive controls for each of these senescence markers (shown in red, with Ins in green and DAPI in blue). Data in panels F, G for p21 and I, J for γ -H2AX is from 8 months old C57BL/6J mice treated with single dose STZ (90 mg/kg) and harvested on day 4 to reflect acute islet stress and DNA damage. Data in panels L, M for p16 is from 8 months old C57BL/6J mice, while the data in panels O, P for LmnB1 is from 8 weeks old NOD female mice prior to any apparent infiltrate and the onset of autoimmune diabetes. For each quantification, 1500 beta cells were counted per pancreas, for $n=4$ mice. (Q) Brightfield and immunofluorescence single channel and merged representative images for senescence marker SA-beta-galactosidase (SA-b-gal, bright field blue) along with TH (red) and Insulin (green), with DAPI (blue), in pancreas tissue from 2 months old wildtype mice. Panel labeled “positive control” shows a representative image from a 1 year old wildtype animal showing senescent cells labeled with SA-b-gal in blue. (R) Quantification for SA-b-gal ($n=4$ mice, 2 months old) in TH+ and TH- beta-cells showing no senescent cells in either population. (S) Boxplots comparing the gene expression of various senescence gene categories (core, effector, and senescence associated secretory phenotype (SASP) genes), between the TH+ and TH- cells of the major beta cell clusters among the three replicate samples presented in Figure 3. The dots represent the outlier cells with gene expression beyond 1.5 times the interquartile range above the upper quartile. Expressions beyond the dotted horizontal line is considered as significant. All panels show representative or mean data from wildtype C57BL/6J mice, with error-bars showing standard error (SEM) of the mean. ns= not significant using 1-way ANOVA with Bonferroni post-hoc test for (B, D), and a paired t -test for (J). Scale bar: 50 μ m.

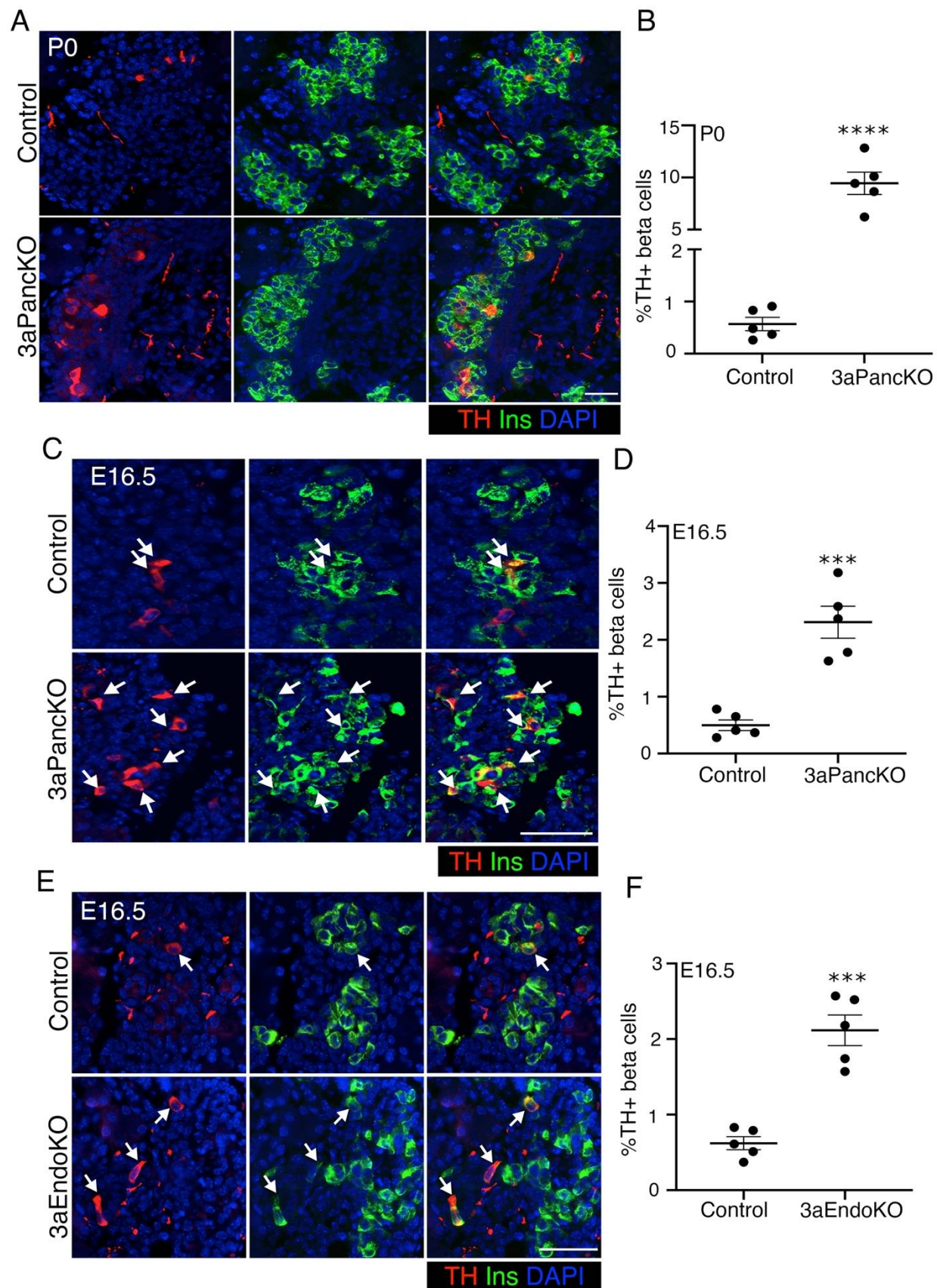


Supplementary Figure 5 (Related to Figure 5). TH promoter undergoes Dnmt3a dependent methylation during the differentiation of endocrine progenitors to beta cells. (A, B) Bisulfite sequencing analysis of the proximal *Th* promoter (-21 to -244 bp region) or -4K region of the *Th* promoter, in purified mouse embryonic pancreatic progenitors, endocrine progenitors, and beta cells, showing the methylation of *Th* promoter during beta cell specification. Each horizontal line with dots represents an independent clone and 10 clones are shown here; with filled circles representing a methylated CpG, while an open circle denotes an unmethylated CpG residue. (C, D) TH expression (green) analysis using immunofluorescence in the developing wildtype embryonic pancreas; in pancreatic progenitors marked by Pdx1 (red) at E12.5 (C), and endocrine progenitors marked by Ngn3 (red) at E13.5 (D). DAPI marks nuclei in blue. (E) Chromatin immunoprecipitation (ChIP) analysis showing the enrichment for repressive histone modification H3K9me3 (filled squares) or IgG control (open squares) to the -2K region of *Th* promoter in sorted embryonic pancreatic- and endocrine-progenitors. Panels (A, B) show representative data from one of the n=3 independent cell preparations, each preparation being a pool of cells derived from multiple embryos. Panels (C, D) show representative examples of data from n=5 independent pancreatic samples. Panel (E) shows data as mean of n=3 independent samples per group, each sample being a pool of cells derived from multiple embryos, with error-bars showing standard error (SEM) of the mean. *** $P < 0.005$, using 1-way ANOVA followed by a Bonferroni post-hoc test. Scale bar: 50 μ m.

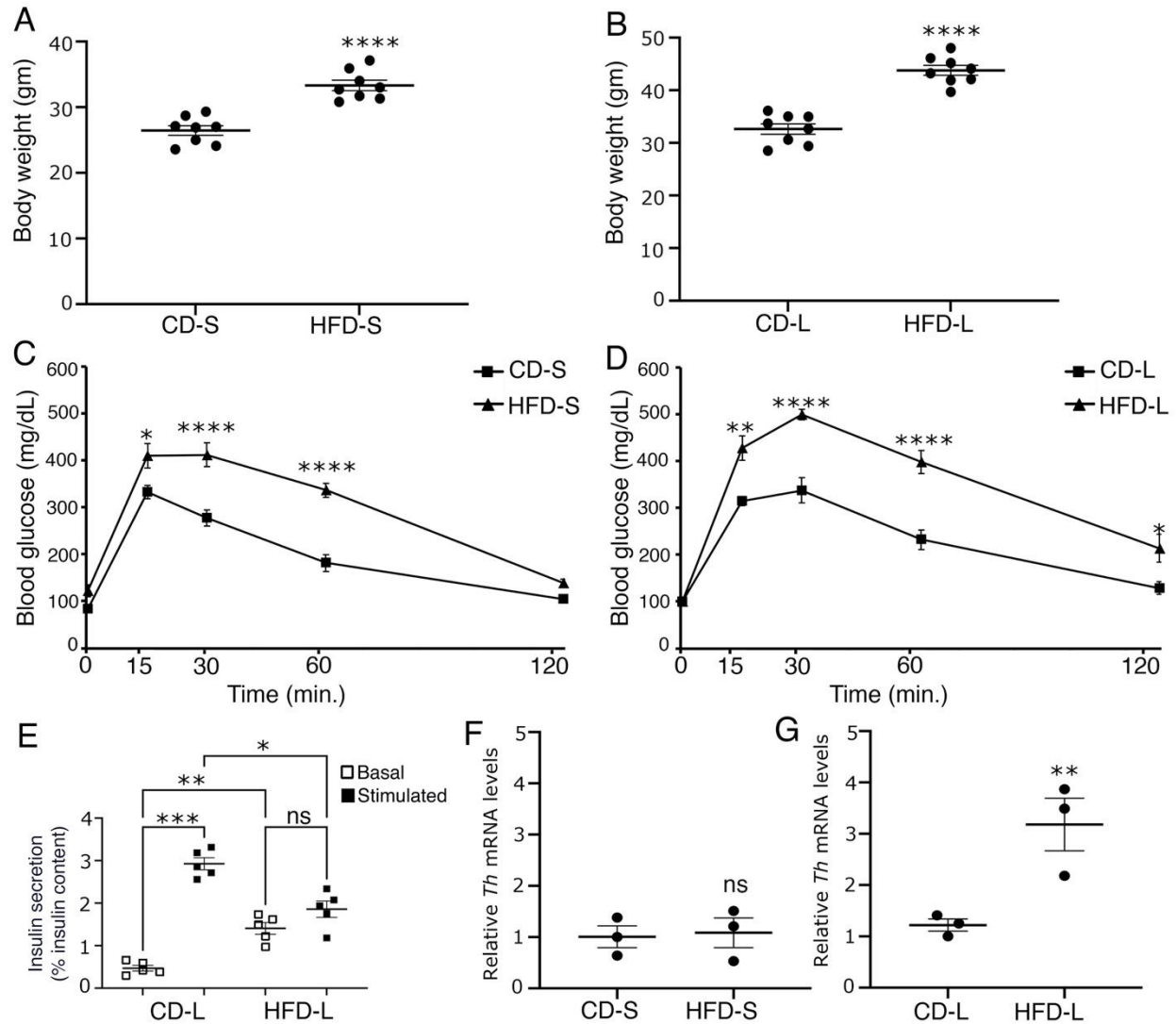


Supplementary Figure 6 (Related to Figure 6). (A-C) Immunofluorescence analysis of TH expression (red) along with lineage specific fluorescent label (GFP or YFP: green) in pancreatic sections from adult (2.5 months old) mice with *Dnmt3a* ablation at various stages of pancreas development and littermate controls, to show efficiency of Cre-recombination as marked by GFP or YFP. Cre recombination in pancreatic progenitor (3aPancKO, A) and beta cell lineage (3aBetaKO, C) is marked by Cre-driven *Rosa26R-YFP*, while Cre recombination in the endocrine progenitor lineage (3aEndoKO, B) is marked by Cre-driven *Rosa26R-mTmG*. Insets shows a 2X magnified view of examples areas marked by white boxes. (D-F) Immunofluorescence analysis of *Dnmt3a* expression (red) along with TH (green) in pancreatic sections from neonatal (P5) mice to

confirm Dnmt3a ablation in 3aPancKO, 3aEndoKO, and 3aBetaKO models. Insets shows a 2X magnified view of examples areas marked by white boxes. We chose neonatal samples to confirm Dnmt3a ablation as Dnmt3a expression declines dramatically after weaning. (G, H) Representative immunofluorescence images (G) and quantification (H) for Insulin (Ins; red), YFP (green), and DAPI (blue) in pancreatic sections from *Ins1Cre: Rosa26 YFP* lineage reporter line, showing good Cre efficiency indicated by overlap of majority of beta cells with Cre driven YFP. Control indicates Cre negative *Rosa26-YFP* littermate. 1200 beta-cells/pancreas, n=5 pancreas. (I, J) Beta-cell mass (I) and static-incubation glucose stimulated insulin secretion (GSIS, isolated islets) (J) in 2.5 months old 3aEndoKO and control littermate mice (n=5 for beta cell mass, n=4 for GSIS), showing no change in beta-cell mass but impaired GSIS response in the KO mice. (K, L) Immunostaining (K) and quantification (L) for TH (red) and glucagon (Glu; green), with DAPI in blue, in pancreatic sections from 2.5 months old 3aPancKO and control mice, showing no overlap of TH and glucagon. 700 alpha-cells/pancreas, n=5 pancreas. (M, N) Immunostaining (M) and quantification (N) for TH (red) and somatostatin (SS; green), with DAPI (blue) in pancreatic sections from 2.5 months old 3aPancKO and control mice, showing increased number of TH+ delta cells (marked by arrows) in the 3aPancKO mice. 700 delta-cells/pancreas, n=5 pancreas. All panels show representative immunofluorescence examples from at least n=5 independent pancreatic samples. The error bars represent standard error (SEM) of the mean. ns= not significant, * $P<0.05$, ** $P<0.01$, determined by using a two-tailed Student's *t*-test for (H, I, L, N) and 1-way ANOVA followed by a Šídák post-hoc test for (J). Scale bar: 50 μ m.



Supplementary Figure 7 (Related to Figure 7). (A, B) Immunofluorescence analysis (A) and quantification (B) of TH expression in pancreatic sections from neonatal mice at P0 with Dnmt3a ablation in pancreatic progenitors (3aPancKO) along with age-matched littermate controls at indicated ages. TH is shown in red, insulin (Ins) in green, and nuclei are labeled by DAPI in blue. Immunofluorescence data shows representative examples from n=5 samples for P0 mice. For quantification, we counted 700 beta-cells/pancreas, n=5 pancreas. (C-F) Immunofluorescence analysis (C, E) and quantification (D, F) of TH expression (red) with insulin (Ins: green) and DAPI (blue) in pancreatic sections from mouse embryos at E16.5 with Dnmt3a ablation in pancreatic (3aPancKO, panels C, E) and endocrine (3aEndoKO, panels D, F) progenitors along with age-matched littermate controls. Nuclei are labeled by DAPI in blue. Arrows mark cells co-expressing TH and insulin. Data shows representative immunofluorescent images and quantification from n=5 KO and littermate control embryos or mice for each group, with 250 beta-cells/pancreas counted,. Error-bars show standard error (SEM) of the mean. *** $P < 0.005$, *** $P < 0.001$, determined by using a two-tailed Student's t -test. Scale bar: 50 μm .



Supplementary Figure 8 (Related to Figure 8). (A-D) Body weight (A, B) and intra-peritoneal glucose tolerance tests (IP-GTT) (C, D) in adult wildtype 7 weeks old mice fed with a high fat- or control-diet for a short term of 8 weeks (HFD-S or CD-S; panels A, C), or long-term for 16 weeks (HFD-L and CD-L; panels B, D). (E) Static incubation GSIS in islets isolated from adult wildtype 7 weeks old mice fed with HFD or control diet for 16 weeks (HFD-L and CD-L), showing impaired GSIS response upon chronic HFD treatment. (F, G) levels of *Th* mRNA relative to housekeeping gene *Cyclophilin*, comparing CD-S vs HFD-S (F), or CD-L vs HFD-L (G) cohorts. For (A-D), n=8 animals. For (F, G), n=3 animals. The error bars represent standard error (SEM) of mean. ns= *P* value not significant (>0.05), * $P<0.05$, ** $P<0.01$, *** $P<0.005$, **** $P<0.001$, determined by using a two-tailed Student's *t*-test for body weight measurements (A, B) and mRNA levels (F, G), and 1-way ANOVA followed by Bonferroni (C, D) and Šídák (E) post-hoc tests.

Supplemental Table 1**Clinical Characteristics of human subjects (Organ donors)**

Fasting Plasma Glucose not available, C-peptide levels are shown where available.

| Status | Age (Year) | Sex | BMI | C-peptide ng/mL |
|--|---------------|-----|-----------|--------------------|
| Fetus Non-diabetic | 16 weeks p.c. | - | - | - |
| Fetus Non-diabetic nPOD 6201 | 36 weeks | M | - | - |
| Neonatal Non-diabetic nPOD 6183 | 0.3 years | M | - | - |
| Neonatal Non-diabetic nPOD 6309 | 0.3 years | M | - | - |
| Neonatal Non-diabetic nPOD 6313 | 0.25 years | M | - | - |
| Adult Non-diabetic nPOD 6057 (quantified) | 22 years | M | 26 | 16.23 |
| Adult Non-diabetic nPOD 6017 (quantified) | 59 years | F | 24.8 | Not available |
| Adult Non-diabetic nPOD 6140 (quantified) | 38 years | M | 21.7 | Not available |
| Adult Non-diabetic nPOD 6030 (qualitative) | 30.1 years | M | 27.1 | Not available |
| Adult Non-diabetic nPOD 6004 (qualitative) | 33 years | M | Not known | Not available |

Supplemental Table 2

Antibodies used for immunofluorescence analyses

| Antibody | Dilution | Source and Catalog Number |
|---|----------|--|
| Mouse anti-Glucagon | 1:1000 | Sigma-Aldrich G2654-.2ML |
| Rabbit anti-Glucagon | 1:500 | Immunostar 20076 |
| Guinea pig anti-Insulin | 1:800 | Abcam 195956 |
| Rabbit anti-insulin | 1:20,000 | Abcam ab181547 |
| Rat anti-somatostatin | 1:300 | Millipore-Sigma MAB354 |
| Mouse anti-Nkx6.1 | 1:50 | Developmental Studies Hybridoma Bank F55A1-0S |
| Mouse anti-Pdx1 | 1:200 | Developmental Studies Hybridoma Bank F109-D12-S |
| Rabbit anti-MafA | 1:500 | Bethyl Laboratories A300-611A |
| Goat anti-NeuroD1 | 1:200 | R&D Systems AF2746 |
| Mouse anti-Ki67 | 1:100 | BD Biosciences 550609 |
| Rabbit anti-pHH3 | 1:200 | Millipore-Sigma 06-570 |
| Mouse anti-Mcm2 | 1:500 | BD Biosciences 610701 |
| Rabbit anti-p21 | 1:500 | Abcam ab188224 |
| Rabbit anti-p16 | 1:500 | Abcam ab211542 |
| Rabbit anti-phospho histone H2AX (γ H2AX) | 1:500 | Cell Signaling 9718S |
| Rabbit anti-LaminB1 | 1:1000 | Cell Signaling 17416 |
| Mouse anti-Dnmt3a | 1:200 | Novus Biologicals NB120-13888 |
| Rabbit anti-Ucn3 | 1:1000 | Gift from Dr. Mark O. Huising, UC Davis |
| Rabbit anti-Ero1b | 1:1500 | Gift from Dr. David Ron, University of Cambridge |
| Mouse anti-TH | 1:200 | Millipore-Sigma MAB318 |
| Rabbit anti-TH | 1:500 | Abcam ab112 |
| Chicken anti-TH | 1:200 | Abcam ab76442 |
| Mouse anti-Tuj1 | 1:500 | Biologend 801201 |
| Chicken anti-GFP | 1:250 | Aves Labs Inc. 1020 |
| Goat anti-PECAM1 | 1:200 | R&D Systems AF3628 |

Supplemental table 3

Antibodies used for ChIP analyses

| Antibody | Source and Catalog Number |
|---------------------|-------------------------------|
| Mouse anti-Dnmt3a | Novus Biologicals NB120-13888 |
| Rabbit anti-H3K9me3 | Millipore-Sigma 07-442 |
| Mouse IgG control | Diagenode KCH-819-015 |
| Rabbit IgG control | Diagenode KCH-504-250 |

Supplemental Table 4

Primers used for ChIP analysis

| Region | Location | Forward | Reverse |
|---------------------------------|--------------------|--------------------------------|--------------------------------|
| <i>Th</i> | -2250 to -1981 bp. | 5' - CCCACCTAGCTTCTGTTGCA - 3' | 5' - CAGGGTAGGACGGAGCTGTA - 3' |
| <i>C (Arx) Negative control</i> | +1348 to +1470 bp. | 5' - AGTGCCCTCTTGCTACCTT - 3' | 5' - TAGGGTGGGGCAAATTTTTA - 3' |

Supplemental Table 5

Primers used for Bisulfite sequencing analysis

| Region | Location | Forward | Reverse |
|-----------------------------|--------------------|--|--------------------------------------|
| <i>Th proximal promoter</i> | -215 to +9 bp. | 5' - GAGGGTGATTTAGAGGTAGGTGTT - 3' | 5' - TATCTCCACAACCCTTACCAAAC - 3' |
| <i>Th -2K</i> | -2250 to -1981 bp. | 5' - GAGTTTAGATATAGATAAAGGTTTGGAGAG - 3' | 5' - ATAAAACAAACCCAACTAAATTCC - 3' |
| <i>Th -4K</i> | -4691 to -4488 bp. | 5' - AGGGTTTAGAGTTAGGGTTGAGATA - 3' | 5' - ATCAAAACCAAATACCAAAACAATTA - 3' |

Supplemental Table 6

Primers used for Real-time qRT-PCR

| Gene | Forward | Reverse |
|--------------------|----------------------------------|------------------------------------|
| <i>Dnmt1</i> | 5' - CAAATAGATCCCCAAGATCCAG - 3' | 5' - CGGAACTAGGTGAAGTTTCAAAAA - 3' |
| <i>Th</i> | 5' - TGTTGGCTGACCGCACAT - 3' | 5' - GCCCCAGAGATGCAAGTC - 3' |
| <i>Cyclophilin</i> | 5' - GTTGGCCAGGCTGGTGTCCAG - 3' | 5' - CTGTGATGAGCTGCTCAGGGTGG - 3' |

Supplementary Methods

Mice

C57BL/6J mice (8 months old) were treated with a single dose of 90 mg/kg Streptozotocin (STZ) using intraperitoneal injections and pancreas harvested on day 4 (3). NOD/ShiLtJ female mice were purchased from Jackson Laboratories (JAX 001976) and pancreas harvested at 8 weeks of age. Pancreas was processed for histology as described in the main methods.

FLIM Imaging

NAD(P)H was excited with a Spectra-Physics Insight 3X ultrafast IR laser at 740 nm, 0.8mW average power, and 4 frame accumulations per optical section, 440-500nm emission. The Alexa dyes were excited using an 860 nm wavelength with the same Spectra-Physics laser. Images were taken at 1024×1024 resolution for N= 3 biological samples and >8 islets/sample. To analyze the metabolic signatures for each beta-cell type, masks for regions of beta-cells were created from fluorescent images of TH and insulin staining respectively by thresholding. Masks (TH+INS+ and TH-INS+) were then preprocessed to fill the cytoplasm of cells and exclude the nuclei. Each mask was applied to the field of view to extract lifetime information from TH+ and TH- cells separately. Paired *t*-test was used to determine significant differences between the two populations.

ScRNA-seq analysis

The datasets were subjected to quality control (elimination of cells with RNA features < 200 or > 10,000 and mitochondrial RNA > 15%) and normalization (“LogNormalize” with scale factor 10,000) in Seurat 4.1 (4) retaining the top 2000 variable genes, followed by integration using the Seurat workflow (5). The integrated data was scaled and subjected to principal component analysis (PCA), following by clustering using the top 15 PCs. The cell types were assigned via the SingleR package (6), using annotated data from mouse pancreatic cells as reference (7). The identified cell types were validated by comparing the expressions of known cell type specific biomarkers. The b-cells were further filtered for low expressions of a- and d-cell markers. b-cells with *Th* expression > 0 were classified as *Th*+. The differential gene expressions were determined using the FindMarkers function in Seurat. For Genset enrichment analysis (GSEA), the differentially expressed genes were ranked according to their adjusted *p*-values, with signs based on the direction of the fold change. GSEA were performed for the Gene Ontology biological process terms (8-10) using the R package ClusterProfiler (11). The enrichment and pathway module plots were prepared using the DOSE (12) and the enrichplot (13) R packages respectively. The volcano plots were prepared using the R package EnhancedVolcano (14).

References

1. Shrestha S, Saunders DC, Walker JT, Camunas-Soler J, Dai XQ, Haliyur R, Aramandla R, Poffenberger G, Prasad N, Bottino R, Stein R, Cartailier JP, Parker SC, MacDonald PE, Levy SE, Powers AC, Brissova M: Combinatorial transcription factor profiles predict mature and functional human islet alpha and beta cells. *JCI Insight* 2021;6
2. Mawla AM, Huising MO: Navigating the Depths and Avoiding the Shallows of Pancreatic Islet Cell Transcriptomes. *Diabetes* 2019;68:1380-1393
3. Tschen SI, Dhawan S, Gurlo T, Bhushan A: Age-dependent decline in beta-cell proliferation restricts the capacity of beta-cell regeneration in mice. *Diabetes* 2009;58:1312-1320
4. Hao Y, Hao S, Andersen-Nissen E, Mauck WM, Zheng S, Butler A, Lee MJ, Wilk AJ, Darby C, Zager M, Hoffman P, Stoeckius M, Papalexi E, Mimitou EP, Jain J, Srivastava A, Stuart T, Fleming LM, Yeung B, Rogers AJ, McElrath JM, Blish CA, Gottardo R, Smibert P, Satija R: Integrated analysis of multimodal single-cell data. *Cell* 2021;184:3573-3587.e3529
5. Stuart T, Butler A, Hoffman P, Hafemeister C, Papalexi E, Mauck WM, 3rd, Hao Y, Stoeckius M, Smibert P, Satija R: Comprehensive Integration of Single-Cell Data. *Cell* 2019;177:1888-1902.e1821
6. Aran D, Looney AP, Liu L, Wu E, Fong V, Hsu A, Chak S, Naikawadi RP, Wolters PJ, Abate AR, Butte AJ, Bhattacharya M: Reference-based analysis of lung single-cell sequencing reveals a transitional profibrotic macrophage. *Nature Immunology* 2019;20:163-172
7. Baron M, Veres A, Wolock SL, Faust AL, Gaujoux R, Vetere A, Ryu JH, Wagner BK, Shen-Orr SS, Klein AM, Melton DA, Yanai I: A Single-Cell Transcriptomic Map of the Human and Mouse Pancreas Reveals Inter- and Intra-cell Population Structure. *Cell Syst* 2016;3:346-360.e344
8. Carlson M: org.Mm.eg.db: Genome wide annotation for Mouse. R package version 3.8.2., 2019
9. Ashburner M, Ball CA, Blake JA, Botstein D, Butler H, Cherry JM, Davis AP, Dolinski K, Dwight SS, Eppig JT, Harris MA, Hill DP, Issel-Tarver L, Kasarskis A, Lewis S, Matese JC, Richardson JE, Ringwald M, Rubin GM, Sherlock G: Gene ontology: tool for the unification of biology. The Gene Ontology Consortium. *Nature genetics* 2000;25:25-29
10. Collaborators GOC: The Gene Ontology resource: enriching a GOLD mine. *Nucleic Acids Res* 2021;49:D325-d334
11. Yu G, Wang L-G, Han Y, He Q-Y: clusterProfiler: an R Package for Comparing Biological Themes Among Gene Clusters. *OMICS: A Journal of Integrative Biology* 2012;16:284-287
12. Yu G, Wang L-G, Yan G-R, He Q-Y: DOSE: an R/Bioconductor package for disease ontology semantic and enrichment analysis. *Bioinformatics* 2014;31:608-609
13. Yu G: enrichplot: Visualization of Functional Enrichment Result. R package version 1.14.2. 2022
14. Blighe K, Rana S, Turkes E, Ostendorf B, Grioni A, Lewis M: EnhancedVolcano: Publication-ready volcano plots with enhanced colouring and labeling. R package version 1.12.0, <https://github.com/kevinblighe/EnhancedVolcano>., 2021